Materials Letters 321 (2022) 132414

Contents lists available at ScienceDirect

Materials Letters

journal homepage: www.elsevier.com/locate/matlet

Strain-dependent phase transformation mapping of diffusion-bonded nanocrystalline aluminum-magnesium by high-energy synchrotron X-rays

Jae-Kyung Han [a], Kunihisa Sugimoto [b,1], Megumi Kawasaki [a,*], Klaus-Dieter Liss [c,*]

[a] School of Mechanical, Industrial and Manufacturing Engineering, Oregon State University, Corvallis, OR 97331, USA
[b] Japan Synchrotron Radiation Research Institute, Sayo-gun, Hyogo 679-5198, Japan
[c] Materials Science and Engineering Department, and Guangdong Provincial Key Laboratory of Materials and Technologies for Energy Conversion, Guangdong Technion – Israel Institute of Technology, Shantou, Guangdong 515063, China

ARTICLE INFO

Keywords:
Aluminum alloy
Heterostructure
High-energy X-rays
High-pressure torsion
Phase transformation

ABSTRACT

This study highlights the capability of high-energy synchrotron X-rays to investigate polymorphous phase transformation upon nanostructuring and diffusion bonding of Al and Mg through high-pressure torsion. The measurements providing diffraction peak profiles at a series of local positions over the sample volume allow mapping of gradual yet significant structural changes in the Al-Mg nanocrystalline alloy. The diffraction peaks involve apparent grain refinement broadening and compositional broadening with increasing shear strain. The results reveal strain-dependent transformations between *f.c.c* and *h.c.p.* phases with a sharp dissolution at strains of ~2500 and subsequent homogenization towards the formation of an Al supersaturated solid solution with the Mg concentration of ~14–15 at.%.

1. Introduction

Metastable and heterogeneous microstructures are under present worldwide research focus to produce advanced structural metals and materials with excellent mechanical and physical properties in a sustainable manner [1]. Nanostructuring through the application of severe plastic deformation has been largely discussed in the modern community [2]. It includes the recent success in the synthesis of aluminum-magnesium (Al-Mg) metastable nanocrystalline alloy through diffusion-bonding of separate Al and Mg sheets at room temperature by high-pressure torsion (HPT) [3,4]. However, the formation of true-nanostructure remains challenging-observations from the understating of structural evolution when involving polymorphous phase transformation. The present study demonstrates a position-resolved 2D texture and structural mapping by high-energy synchrotron X-rays, revealing concurrent structural changes towards the formation of a metastable nanocrystalline state in a supersaturated solid solution through HPT-induced diffusion bonding.

2. Experimental

Diffusion bonding of Al (Al-1050) and Mg (ZK60) disks with 10 mm diameter and ~ 0.83 mm thicknesses in the stacking order of Al/Mg/Al was conducted at room temperature by HPT under < 6 GPa for 100 revolutions at 1 rpm. While severe plastic deformation at 6 GPa was satisfactory to bond the metals and form a bulk Al metastable alloy with an average supersaturated Mg content of ~ 14.2 at.% [3,4], the present lower pressure of < 6 GPa delays Mg dissolution into Al which can introduce a hierarchical and transitional microstructure. High-energy X-ray diffraction (HEXD) [5] has been performed at beamline BL02B1, SPring-8, Japan. The beam was focused on the sample at 0.2 mm (horizontal) × 0.3 mm (vertical) and calibrated by CeO_2 standard to 72.2515 keV, rendering a nominal wave number of $k = 36.5898$ Å^{-1} and wavelength of $\lambda = 0.17172$ Å. A Perkin-Elmer PE XRD 1621 CN3 EHS flat-panel detector of 40 mm side length and 0.200 mm pixel size was centered to record entire diffraction rings. The distance from the specimen was calibrated by triangulation to 909.607 mm. The entire disk specimen was mounted normal to the beam in transmission mode and scanned in a raster with 0.65 mm step size in both lateral dimensions to map diffractograms as a function of position. Two-dimensional detector images were sectored into 48 radial diffractograms, allowing to account for the azimuthal anisotropy, such as texture and strain, within the sample [6]. The schematic sample set up and the HEXD measurement locations are shown in Fig. 1.

* Corresponding authors.
E-mail addresses: megumi.kawasaki@oregonstate.edu (M. Kawasaki), kdl@gtiit.edu.cn, liss@kdliss.de (K.-D. Liss).
[1] Currently at: Department of Chemistry, Kindai University, Higashi-Osaka, Osaka 577-8502, Japan.

https://doi.org/10.1016/j.matlet.2022.132414
Received 3 May 2022; Accepted 4 May 2022
Available online 6 May 2022

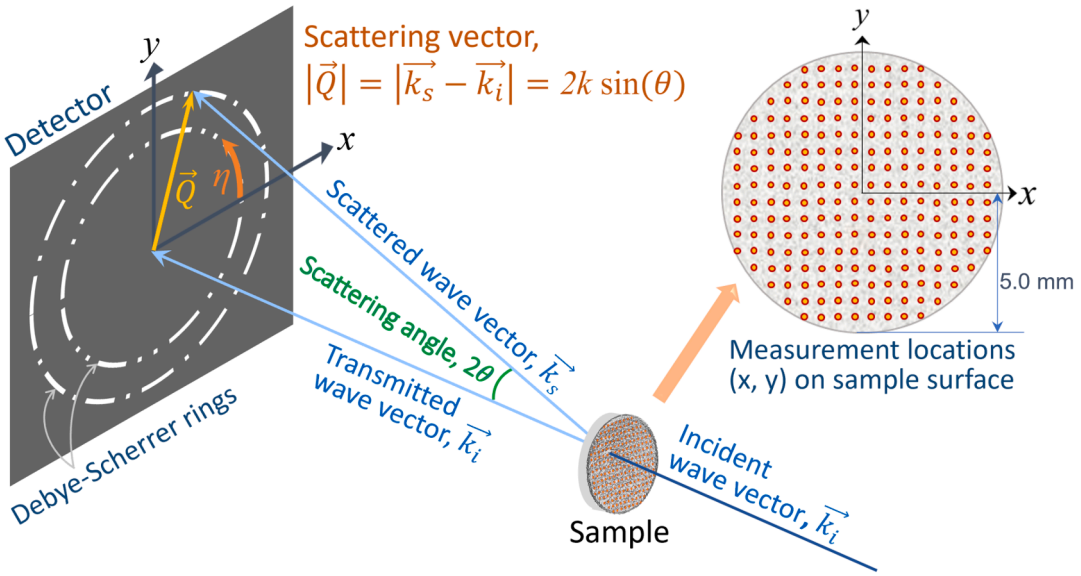

Fig. 1. Schematic sample set-up and the HEXD measurement locations.

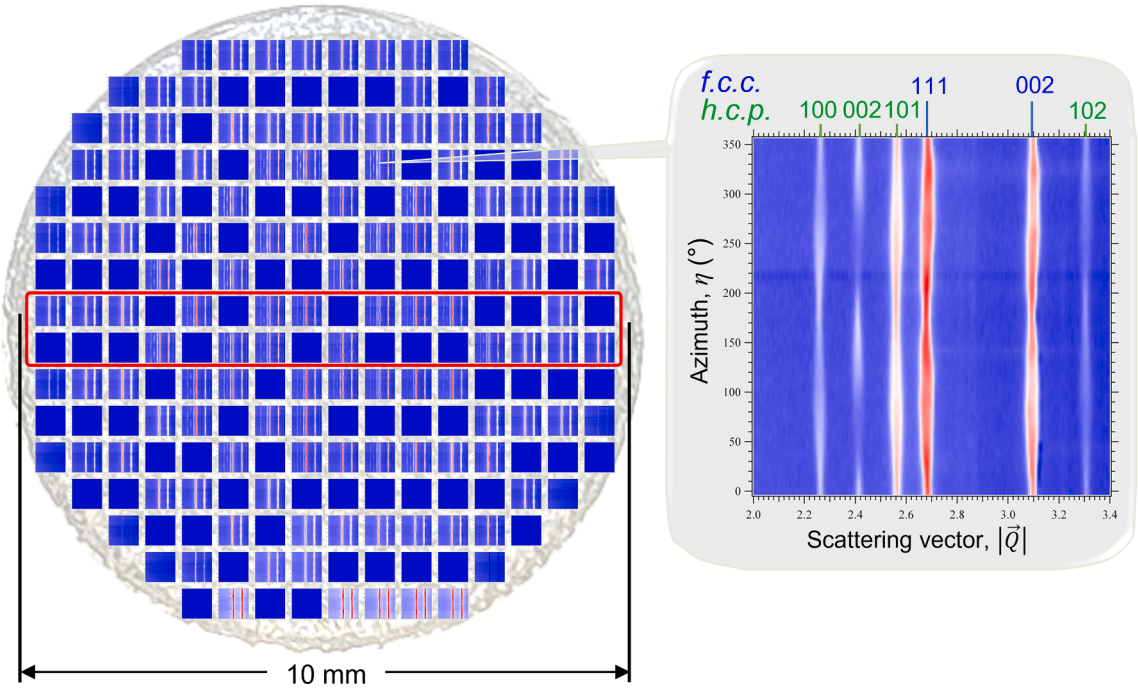

Fig. 2. Position-dependent structure map constructed by a series of the HEXD patterns with an enlarged representative diffractogram.

3. Results and discussion

Fig. 2 shows a series of the HEXD patterns at all measurement locations enabling mapping of structure and texture variations for the Al-Mg alloy. Each HEXD diffractogram provides the Debye-Scherrer pattern along azimuth η versus scattering vector $|\vec{Q}|$. The map is superimposed on a photo of the Al-Mg disk, where the disk fringe after processing widens the apparent diameter. The detector failed to collect HEXD data at several local positions, whose maps appear in blue. As seen in the enlarged representative plot taken at the mid radius of the sample, the HEXD patterns with increasing relative peak intensity exhibit a color change from white to red in the blue background. There is a mixture of Al-rich and Mg-rich phases having face-centered cubic (*f.c.c.*) and hexagonal (*h.c.p.*) close-packed structures, respectively, and each peak shows a unique azimuthal intensity distribution, thereby implying the formation of ultrafine grains having preferred crystallographic orientations. There is no trace of any intermetallic compound at any local locations within the sample. The principles of HPT processing [7] describe total shear strain as $\gamma = 2\pi Nr/h$, where N is the revolution number, r is the distance from the disk center, and h is the initial sample thickness. The map describes an overall view of the strain-dependent crystallographic characteristics and phase transformation.

The region surrounded by a red box in Fig. 2 was further examined for polymorphous phase transformation during diffusion bonding of the *f.c.c.* and *h.c.p.* phases. Considering radial symmetry of the strain distribution leading to gradient nanostructuring within HPT samples, Fig. 3

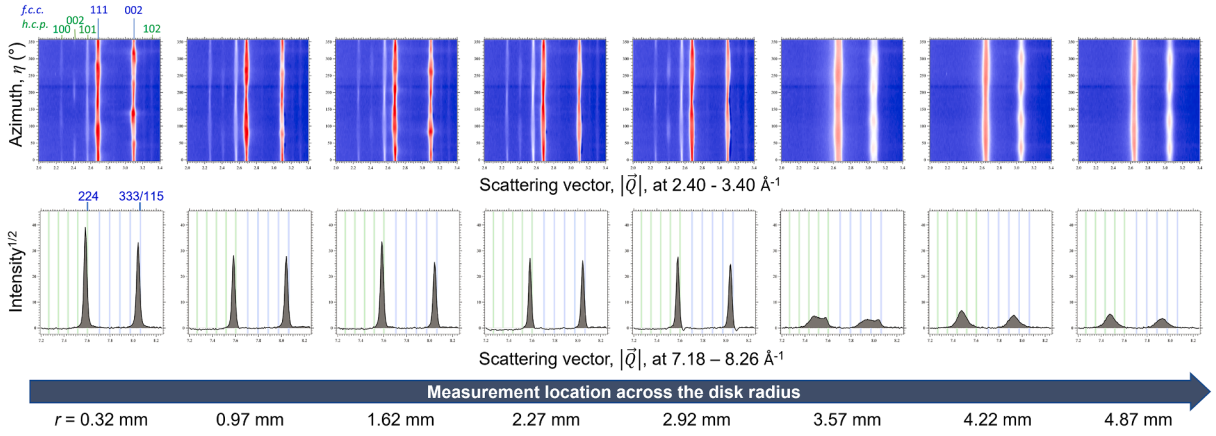

Fig. 3. Phase transformation shown by the HEXD maps (upper row) and the HEXD patterns for *f.c.c.* phases integrated at $\eta = 323.5–360.0°$ at high $|\vec{Q}|$ (lower row) across the disk radius.

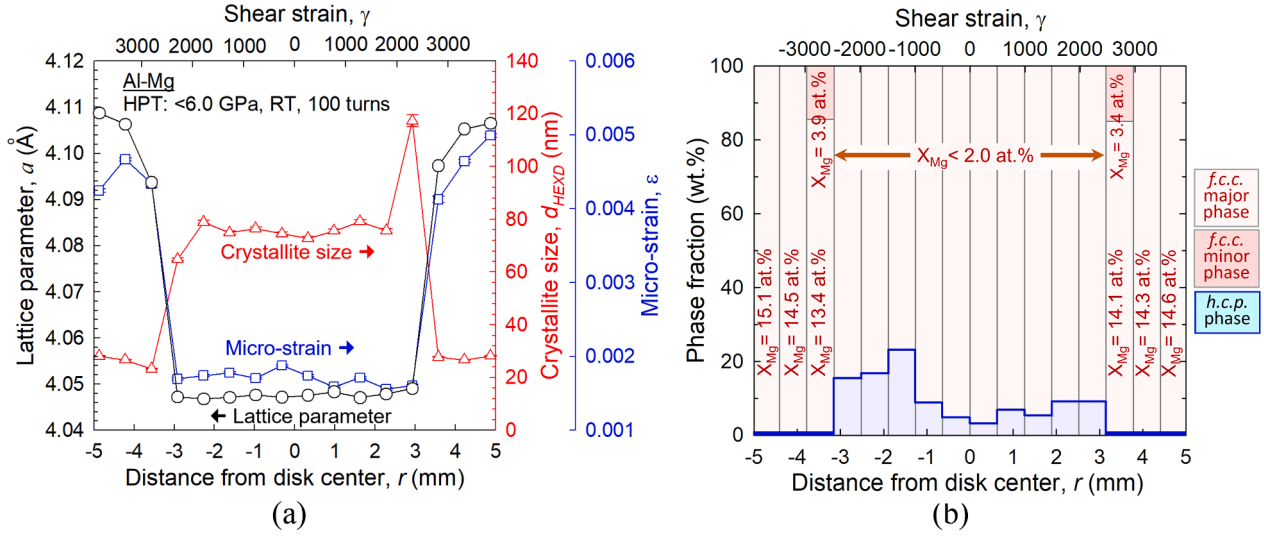

Fig. 4. The strain-dependent structural changes observed by the HEXD experiments for (a) lattice parameter, crystallite size, and micro-strain for a major *f.c.c.* phase, and (b) phase fractions of the *f.c.c.* and *h.c.p.* phases.

illustrates a series of the HEXD plots (upper row) and position-sensitive diffractograms for the *f.c.c.* phases integrated at $\eta = 323.5–360.0°$ at high $|\vec{Q}|$ (lower row) across the disk radius. The $|\vec{Q}|$ range captures the 224 and 333/115 reflections of the *f.c.c.* phases with wide apparent peak broadening. The green and blue lines at $|\vec{Q}| = 7.6165$ and 8.0785 Å^{-1}, respectively, indicate the peaks at those reflections for pure Al with a lattice parameter of $a_0 = 4.0414$ Å [8]. Thus, any peak shift from the pure metal provides, following Vegard's law and an empirical relationship [9], the estimation of the Mg content, given as $X_{Mg} = \{9.045[(a - a_0)/a_0] \pm 0.003\} \times 100$ in at.%, where a is the lattice constant of the observed *f.c.c.* phase. The second to fifth green and blue lines toward lower $|\vec{Q}|$ indicate X_{Mg} of 10, 20, 30 and 40 at.% at 224 and 333/115 indices, respectively.

The HEXD maps prove that an *h.c.p.* phase is visible at $r < 3$ mm, while disappearing at $r > 3$ mm. The *f.c.c.* peaks show strong azimuthal modulation in the less broadened *f.c.c.* diffractograms at lower r, while such azimuthal intensity was dispersed in wider η and the overall HEXD peak widths are broadened in $|\vec{Q}|$ at higher r. Apparent differences in shape and position are visible in the HEXD profiles for the *f.c.c.* phases at high $|\vec{Q}|$. Specifically, the peaks at 224 and 333/115 indices are sharp and less broadened with peak positions suggesting close to pure Al at $r <$ 3.0 mm. For $r > 3.0$ mm, these are widely broadened and shifted in peak position, implying high dissolution of Mg into the *f.c.c.* phases with different concentrations. Moreover, at $r = 3.57$ mm the peaks exhibit a plateau and double-peak profile suggesting compositional separation. An earlier study for the diffusion-bonded Al-Mg alloy describes such unique peak profiles as grain refinement broadening and compositional broadening [3].

The strain-dependent features in peak broadening of HEXD are quantitatively analyzed across the disk diameter. The results are summarized in Fig. 4 for (a) lattice parameter a, crystallite size d_{HEXD}, and micro-strain ε for a major *f.c.c.* phase, and (b) fractions of the *f.c.c.* and *h.c.p.* phases. (Data available in Supplementary Table S1) These structural parameters are estimated using the MAUD Rietveld analysis package [10], where HEXD peak broadening by grain refinement is considered as a function of d_{HEXD} and ε. Compositional broadening shifting the diffraction peaks yields the different a through MAUD for the existing *f.c.c.* phases, which further estimate X_{Mg}. The *f.c.c.* and *h.c.p.* phase fractions are also estimated through MAUD.

The results reveal the strain-dependent phase transformation during diffusion bonding and nanostructuring by HPT, where $\gamma \approx 2500$ led to a

minimum d_{HEXD} of ~ 30 nm with increasing a and ε attributing to Mg dissolution into Al. Separate *f.c.c.* and *h.c.p.* phases exist at $\gamma < 2500$, while the *h.c.p.* phase dissolved to produce a supersaturated *f.c.c.* major phase (X_{Mg} = 13–14 at.%) together with an Al-rich *f.c.c.* minor phase (X_{Mg} = 3–4 at.%) at $2500 < \gamma < 3000$. These *f.c.c.* major and minor phases eventually mixed into one Al supersaturated solid solution with X_{Mg} = 14–15 at.% at the disk periphery. All phase changes appear radially symmetric, confirming the strain-dependence of the phase transformation. The achieved values at the disk peripheries are consistent with the reported crystallite size of ~ 25–34 nm and the average Mg concentration of ~ 14.2 at.% in Al in a bulk Al-Mg nanocrystalline metastable alloy [3]. This study demonstrates unique potential of high-energy synchrotron X-ray diffraction for visualization of heterogeneous structural changes and phase transformation in nanostructured metals.

4. Conclusions

Localized measurements using high-energy synchrotron X-rays over the sample volume allows mapping of structural evolution of Al and Mg during nanostructuring and diffusion bonding by HPT. The HEXD peaks for the *f.c.c.* phases show a combination of grain refinement broadening and compositional broadening with increasing shear strain, enabling a detailed evaluation of structural and phase evolution in the alloy. The results reveal gradual yet apparent transformations between *f.c.c* and *h.c.p.* phases towards the formation of a metastable nanocrystalline Al-Mg alloy having $d_{HEXD} \approx$ 30 nm with Mg supersaturation of ~ 14–15 at.%. At strain ~ 2500, the *h.c.p.* phase completely dissolves into a bimodal distribution of the high and low X_{Mg}-concentrated *f.c.c.* phases, which equilibrate at larger strains.

CRediT authorship contribution statement

Jae-Kyung Han: Resources, Investigation, Formal analysis. **Kunihisa Sugimoto:** Investigation. **Megumi Kawasaki:** Supervision, Resources, Writing – original draft. **Klaus-Dieter Liss:** Investigation, Formal analysis, Writing – review & editing.

Declaration of Competing Interest

The authors declare that they have no known competing financial interests or personal relationships that could have appeared to influence the work reported in this paper.

Acknowledgements

This study was supported by the National Science Foundation of the United States under Grant No. DMR-1810343. The authors acknowledge the Japan Synchrotron Radiation Research Institute for granting beam time and logistics on beamline BL02B1 at SPring-8 under Proposal No. 2018B1219.

Data availability

Synchrotron data under Proposal No. 2018B1219 was recorded using SPEC software and corresponding SPEC-file '190201_dieter.dat'. Detector images were taken into the files named 'pe_CcdNum_AverageResult.his'. For the CeO_2 calibration, the scan number is #S5016 with 'CcdNum' of 11565, and those for the reported specimen set has numbers of #S5022-#S5239 with 11729-11946, respectively.

Appendix A. Supplementary data

Supplementary data to this article can be found online at https://doi.org/10.1016/j.matlet.2022.132414.

References

[1] X. Li, K. Lu, Improving sustainability with simpler alloys, Science 364 (6442) (2019) 733–734.
[2] K. Edalati, A. Bachmaier, V.A. Beloshenko, Y. Beygelzimer, V.D. Blank, et al., Nanomaterials by severe plastic deformation: Review of historical developments and recent advances, Mater. Res. Lett. 10 (4) (2022) 163–256.
[3] J.-K. Han, K.-D. Liss, T.G. Langdon, M. Kawasaki, Synthesis of a bulk nanostructured metastable Al alloy with extreme supersaturation of Mg, Sci. Rep. 9 (2019) 17186.
[4] J.-K. Han, K.-D. Liss, T.G. Langdon, J.-I. Jang, M. Kawasaki, Mechanical properties and structural stability of a bulk nanostructured metastable aluminum-magnesium system, Mater. Sci. Eng. A 796 (2020), 140050.
[5] K.-L. Liss, A. Bartels, A. Schreyer, H. Clemens, High-Energy X-Rays: A Tool for Advanced Bulk Investigations in Materials Science and Physics, Textures Microstruct. 35 (2003) 219–252.
[6] K.-D. Liss, K. Yan, Thermo-Mechanical Processing in a Synchrotron Beam, Mater. Sci. Eng. A 528 (1) (2010) 11–27.
[7] A. Zhilyaev, T. Langdon, Using high-pressure torsion for metal processing: Fundamentals and applications, Prog. Mater. Sci. 53 (6) (2008) 893–979.
[8] M.E. Straumanis, The precision determination of lattice constants by the powder and rotating crystal methods and applications, J. Appl. Phys. 20 (1949) 726.
[9] H.L. Luo, C.C. Chao, P. Duwez, Metastable solid solutions in aluminum-magnesium alloys, Trans. Metall. Soc. AIME 230 (1964) 1488–1490.
[10] L. Lutterotti, S. Matthies, H.-R. Wenk, MAUD (Material Analysis Using Diffraction): a user friendly Java program for Rietveld texture analysis and more, Proceeding of the twelfth international conference on textures of materials (ICOTOM-12), 1 (1999) 1599.